



ELSEVIER

Available online at www.sciencedirect.com

SCIENCE @ DIRECT®

Nuclear Instruments and Methods in Physics Research B 200 (2003) 191–195

NIM B
Beam Interactions
with Materials & Atomswww.elsevier.com/locate/nimb

GISAXS studies of morphology and size distribution of CdS nanocrystals formed in SiO₂ by ion implantation

U.V. Desnica^{a,*}, P. Dubcek^a, I.D. Desnica-Frankovic^a, M. Buljan^a,
K. Salamon^b, O. Milat^b, S. Bernstorff^c, C.W. White^d

^a Department of Physics, Rudjer Boskovic Institute, Bijenicka 54, 10000 Zagreb, Croatia

^b Physics Institute, Bijenicka 58, 10000 Zagreb, Croatia

^c Sincrotrone Trieste, SS 14 km 163,5, 34012 Basovizza, Italy

^d Oak Ridge National Laboratory, P.O. Box 2008, Oak Ridge, TN 37831, USA

Abstract

Grazing incidence small angle X-ray scattering (GISAXS) was applied to study the synthesis and size evolution of CdS nanocrystals. CdS was formed in SiO₂ substrate by successive multi-energy implantation of constituent elements (three different ion doses) and subsequent thermal annealing ($T_a = 800$ or 1000 °C). The analysis of 2D GISAXS patterns with the Guinier plot was compared to the fit results of the local mono-disperse approximation. Results indicate that the applied implantation + annealing procedure resulted in formation of isolated, spherical CdS nanoparticles embedded in SiO₂ amorphous matrix, evenly distributed in the substrate in all three dimensions. Nanoparticle average size, size distribution, inter-particle distance and fraction of synthesized atoms were determined. Larger doses induced strong clustering into larger nanoparticles, accompanied with the increase of inter-cluster distance, that indicates the strain-related enhancement of the diffusion of small CdS nanocrystals. Results promote GISAXS as an excellent and nondestructive tool to investigate the role of particular implantation and annealing steps, in term of nanocrystal size, morphology and size distribution of CdS nanocrystals.

© 2002 Elsevier Science B.V. All rights reserved.

PACS: 61.10.Eq; 81.07.-b; 61.72.V; 61.46.+w; 81.20.-n; 81.05.Ys

Keywords: Nanocrystals; Quantum dots; X-ray scattering; SAXS; GISAXS; Implantation; CdS

1. Introduction

There is an intense research activity going on to develop technology for the efficient and controllable synthesis of nanocrystals or quantum dots

(QDs) [1–4]. This interest is mainly due to strong modification of electronic, optical and other properties of QDs with respect to corresponding bulk materials, offering a number of potential applications in semiconductor and other industries [1]. Due to a large surface to volume ratio, QDs are chemically reactive and have to be embedded into an appropriate host material. High-dose implantation is considered to be one of the best methods to produce well-defined buried layers

* Corresponding author. Tel.: +3851-4561-173; fax: +3851-4680-114.

E-mail address: desnica@rudjer.irb.hr (U.V. Desnica).

with a high volume fraction of nanocrystals [4]. Sequential implantation of equal doses of constituent atoms offers a unique way to produce compound-semiconductor QDs [1,3,5]. In particular, the formation of CdS-QDs in SiO₂ after ion implantation of Cd and S atoms was confirmed recently [1,3,5,6]. The main interest in wide band-gap semiconductor QDs comes out from pronounced effects of quantum confinement and from powerful visible photoluminescence, which are strongly dependent on the particle size. Hence, by controlling the particle size the tunability of the band-gap becomes possible. However, optimization of implantation parameters and post-implant procedure, in order to achieve proper size and size distribution in implantation-produced QDs appears to be the most challenging task for this method [1]. In this paper the structure of the implanted layer with CdS QDs was investigated by means of Grazing incidence small angle X-ray scattering (GISAXS).

2. Experimental details

Samples were produced by implanting into amorphous SiO₂ equal doses of Cd and S ions at multiple energies, chosen to form depth profiles of nearly uniform concentration, C , in the surface layer. Three doses of implanted constituent atoms created concentrations of $C1 = 5.3 \times 10^{21}/\text{cm}^3$, $C2 = 2.0 \times 10^{21}/\text{cm}^3$ and $C3 = 0.8 \times 10^{21}/\text{cm}^3$, respectively, in the approximately first 160 nm of SiO₂. The subsequent annealing at either $T1 = 1000$ °C or $T2 = 800$ °C, for 1h in the flow of Ar + 4%H₂, caused diffusion of Cd and S atoms and formation into CdS nanocrystals. GISAXS experiments were carried out with the X-ray wavelength, $\lambda = 0.154$ nm, in Austrian SAXS line at Elettra, Sincrotrone Trieste, Italy. The GISAXS patterns were recorded with a 1024×1024 pixels 2D detector, placed in the y - z plane, (Fig. 1), perpendicularly to specular plane (x - z plane). The smallest grazing angle at which the signal from inside of the film was detected is assumed to be equal to the critical angle. Spectra were first corrected for background intensity and detector response, and then for refraction and absorption effects [7,8].

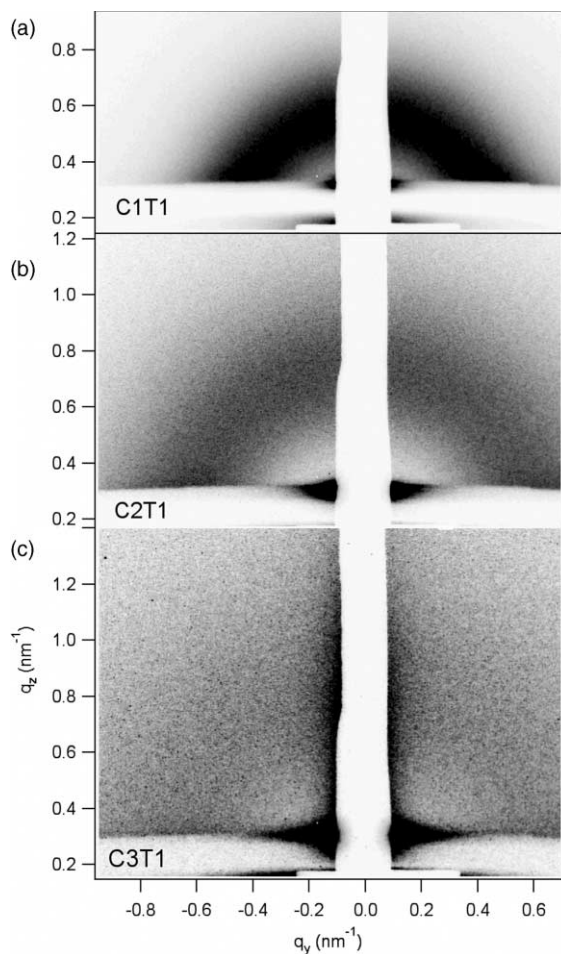


Fig. 1. 2D GISAXS spectra of CdS in SiO₂, obtained by implantation of constituent atoms and subsequent annealing at $T1 = 1000$ °C, for concentration of implanted Cd and S atoms: (a) $C1 = 5.3 \times 10^{21}/\text{cm}^3$, (b) $C2 = 2.0 \times 10^{21}/\text{cm}^3$ and (c) $C3 = 0.8 \times 10^{21}/\text{cm}^3$.

3. Results and discussion

Fig. 1(a)–(c) show 2D GISAXS patterns of CdS nanoparticles in SiO₂ for samples implanted to concentrations $C1$, $C2$ and $C3$, respectively, and subsequently annealed at $T1 = 1000$ °C. Angle of X-ray beam incidence, α , was equal to the critical angle for total external reflection, α_c . The 2D patterns represent maps of the scattering intensities in reciprocal space, q , where q is the wave vector $q = (4\pi/\lambda) \sin \beta$, and 2β is the scattering

angle. In order to block strong surface signals (reflected beam, Yoneda, etc.) in/close to the specular plane, a beam-stopper was inserted, allowing better sensitivity for the weak diffuse scattering at larger q . As the implanted dose increases the total scattering intensity increases and localizes, while the intensity maximum moves toward smaller q . All three GISAXS patterns comprise a highly intense region close to the center (remaining part of surface contributions, which will be ignored in further discussion) and half rings, which are considered as due to scattering from CdS clusters formed in the substrate. After the appropriate corrections were applied, all rings proved to be circular and similar in shape in all directions. So, we can conclude that the combination of implantation and annealing procedures resulted in formation of isolated, spherical CdS nanoparticles, evenly distributed in SiO₂ amorphous matrix in all three dimensions.

Comparative scans of 2D GISAXS spectra along z -axis, offset for the beam-stopper width, are reported in Fig. 2, for all six samples. They show scattering intensity, $I(q)$, versus q along the z -axis. For each dose, C_i , larger and smaller symbols refer, respectively, to the higher and lower annealing temperature T_a ($T1$ and $T2$). There is a clear regularity in the $I(q)$ dependence, whether one compares various doses (for same T_i) or various T_i for the same C_i . Overall, both higher dose and higher T_a cause a shift of the intensity maximum toward lower q as well as steeper decrease of $I(q)$ on the right side of the maximum.

When a simple particle scattering model (Guinier approximation) is applied for the analysis of such GISAXS profiles, the average cluster diameter D is obtained from the radius of gyration, R_g , computed from the slope of the linear region of the $I(q)$ versus q^2 dependence. The average distance among nanocrystals, L , is determined from the position of the interference peak, q_m , as $L = 2\pi/q_m$. Numerical results for R_g and L are given in the inset of Fig. 2. For the lowest dose, $C3$, however, the particle signal is quite weak. For $T_a = 1000$ °C (sample $C3T1$), correlation maximum is still distinguishable, but it is broad and superimposed on relatively strong surface signal, so that the apparent q_m is shifted toward smaller q , giving

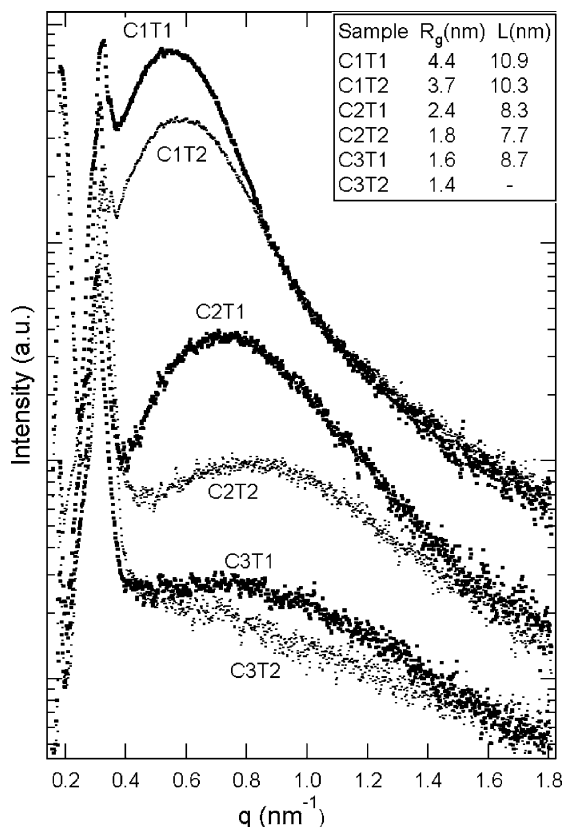


Fig. 2. Specular scans, offset for the beam-stopper width, of 2D GISAXS spectra for three doses, C_i , and two annealing temperatures, T_i . Sample $T1C1$ denotes sample implanted to $C1$ and annealed at $T1 = 1000$ °C, etc.

unrealistically large L . For lower T_a , L could not be determined at all, since the particles were too far apart to correlate.

The well-resolved GISAXS spectra from CdS nanoparticles were obtained for all samples, proving the successful synthesis of CdS QDs for all selected doses and annealing temperatures. Predictably, for a given dose, higher T_a yields larger average R_g , accompanied with somewhat larger L (i.e. QDs are larger and further apart). However, for both $T1$ and $T2$, higher dose also results in an increase of L , although in high-dose samples the density of implanted Cd and S ions is much higher.

Besides the Guinier plot analysis, an analysis of GISAXS spectra based on local mono-disperse approximation (LMA) [9,10] was performed. In LMA approximation, it is assumed that the

positions and the sizes of particles are completely correlated. That is, the system is approximated by many mono-disperse subsystems. The total scattering is calculated as the sum of the scatterings from the subsystems, weighted according to the size distribution of the system. The scattered intensity is [9]:

$$I(q) \propto |T(\alpha_i)|^2 |T(\alpha_f)|^2 \int_0^\infty P(q, D) S(q, D_{\text{hs}}, \eta_{\text{hs}}) \times N(D, w) dD, \quad (1)$$

where $T(\alpha_i)$ and $T(\alpha_f)$ are the Fresnel transmission coefficients for angle of incidence, α_i , and exit, α_f , respectively. $P(q, D)$ is the form factor of a homogeneous sphere of diameter D ; $N(D, w)$ represents (here assumed) Gaussian size distribution function with a full width at half maximum (FWHM), w ; $S(q, D_{\text{hs}}, \eta_{\text{hs}})$ is the structure factor, where η_{hs} and D_{hs} are the volume fraction and diameters of hard spheres. Model assumes that hard sphere includes the ‘precipitate’ of diameter D plus surrounding depleted zone with no other precipitates [10]. Therefore, we consider LMA as a particularly appropriate approach for studying nanocrystals obtained by implantation and subsequent annealing: after implantation atoms are distributed very uniformly, while during annealing nanocrystals grow by depleting the space around them, larger QDs being surrounded by a larger depleted volume.

Fig. 3 shows 1D GISAXS angular spectra (all corrections included) for the same set of samples as in Fig. 1, taken along polar angle 70° , together with their best LMA fits. Fit parameters are given in corresponding insets. Comparing results of Guinier and LMA approximations both methods give similar values for L as well as for D , if one assumes the relation $D = 2R_g$ [9]. Both results are in accordance with our finding that CdS nanoparticles are spherical. Again, not only D but also L increased with the increase of dose, after annealing at the same $T_a = 1000^\circ\text{C}$. Although in sample C1T1, for example, the concentration of implanted cluster-building Cd and S atoms was almost seven times larger than in the sample C3T1 (and implanted atoms were initially much closer to each other), after annealing the synthesized QDs are almost two times further apart in C1T1 than in

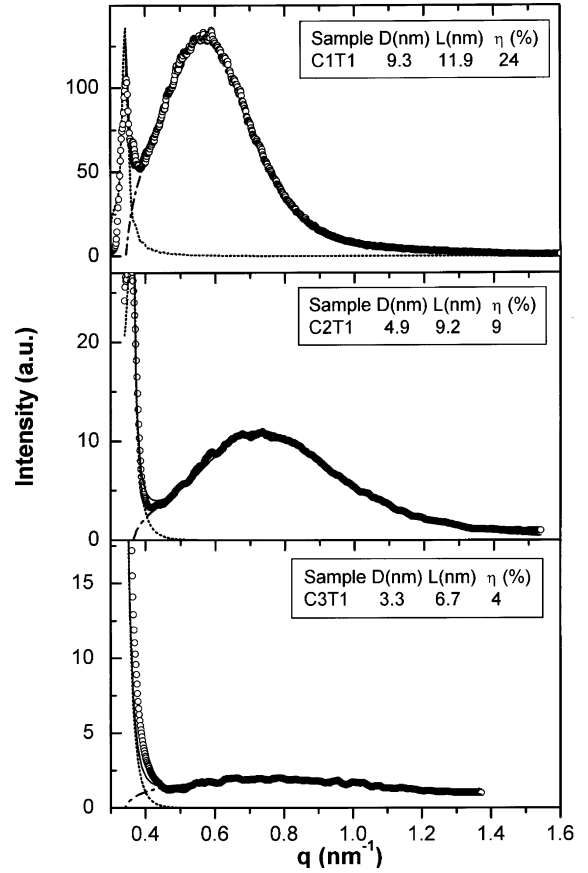


Fig. 3. 1D GISAXS pattern (open circles) of three samples implanted with doses C1, C2 and C3 and annealed at $T_1 = 1000^\circ\text{C}$. The solid line is the best fit of the LMA, dash-dot-dash line represents CdS nanocrystal contribution, and dotted line represents surface effects contribution. Insets show numerical data for average diameter D , average inter-cluster distance L , and CdS volume fraction η , obtained from the best fits.

C3T1. This indicates that higher dose strongly stimulates further clustering of small QDs into larger ones. Result effectively suggests the dose-enhanced diffusion of smaller CdS QDs. Since the presence of larger amount of large foreign atoms is expected to induce larger lattice strain, we assume that the observed enhancement of diffusion is strain-induced. The presence of strain was also suggested by the deformations of observed Moiré fringes in high-dose implanted samples [1].

Presented GISAXS results were compared with the high-resolution TEM results. TEM-determined average diameters of CdS QDs in analogous

samples (implanted with the same three doses and annealed at 1000 °C) were 9.8, 6.5 and 4.9 nm, respectively, [3]. Considering all the differences between GISAXS and TEM techniques, in particular that GISAXS averages over the large part of the sample surface, while TEM probes very locally, giving the projected area of buried clusters, the agreement for D is reasonably good, particularly for larger doses. The LMA-calculated values for FWHM ($w = 6.5, 4$ and 2.7 nm, for $C1, C2$ and $C3$, respectively) agree very well with the ones estimated from TEM nomograms [3]. Furthermore, for all three doses the LMA values for CdS volume fraction in SiO_2 , η , (Fig. 3) are in very good agreement with values calculated under assumption that virtually all implanted Cd and S atoms are indeed synthesized into CdS after 1000 °C annealing. All these results promote GISAXS as an excellent and nondestructive tool to investigate the role of implantation and annealing steps, in quest for the desired size, morphology and size distribution of CdS nanocrystals – and probably other II–VI compounds-, formed by ion implantation of constituent atoms into light matrix.

4. Conclusions

GISAXS was applied to study CdS nanocrystals formed in SiO_2 substrate by successive multi-energy implantation of constituent atoms and subsequent thermal annealing. It has been demonstrated that GISAXS is a very sensitive technique that can be applied successfully to study the synthesis, evolution of average nanocrystal size, size distribution, inter-cluster distances and their distribution as a function of implantation and annealing parameters. Either larger dose or higher T_a result in larger nanocrystals, accompanied with a larger inter-particle distance. In particular, higher doses (at the

same T_a) favor the formation of bigger clusters even if therefore they have to be further apart, indicating the dose-dependent strain-induced enhancement of diffusion of smaller CdS QDs and their clustering into larger particles. Comparison of GISAXS and TEM results for size and size distributions showed reasonably good agreement.

Acknowledgements

This work was supported by the Ministry of Science and Technology, Republic of Croatia. Oak Ridge National Laboratory is managed by UT-Battelle, LLC, for the US Department of Energy under contract DE-AC05-00OR22725.

References

- [1] A. Meldrum, R.F. Haglund Jr., L.A. Boatner, C.W. White, *Adv. Mater. (Rev.)* 13 (2001) 1431.
- [2] J.D. Budai, C.W. White, S.P. Withrow, M.F. Chisholm, J. Zhu, R.A. Zuhr, *Nature* 390 (1997) 384.
- [3] C.W. White, A. Meldrum, J.D. Budai, S.P. Withrow, E. Sonder, R.A. Zuhr, D.M. Hembree Jr., M. Wu, D.O. Henderson, *Nucl. Instr. and Meth. B* 148 (1999) 991.
- [4] H. Karl, I. Grosshans, W. Attenberger, M. Schmid, B. Stritzker, *Nucl. Instr. and Meth. B* 178 (2001) 126.
- [5] U.V. Desnica, O. Gamulin, A. Tonejc, M. Ivanda, C.W. White, E. Sonder, R.A. Zuhr, *Mater. Sci. Eng. C* 15 (2001) 105.
- [6] U.V. Desnica, I.D. Desnica-Frankovic, O. Gamulin, C.W. White, E. Sonder, R.A. Zuhr, *J. Non-Cryst. Solids* 299–302 (2002) 1100.
- [7] M. Buljan, K. Salamon, P. Dubcek, S. Bernstorff, I.D. Desnica-Frankovic, O. Milat, U.V. Desnica, *Vacuum*, in press.
- [8] B. Kutch, O. Lyon, M. Schmitt, M. Mennig, H. Schmidt, *J. Appl. Crystallogr.* 30 (1997) 948.
- [9] D. Babonneau, I.R. Videnovic, M.G. Garnier, P. Oelhafen, *Phys. Rev. B* 63 (2001) 195401.
- [10] R. Triolo, E. Caponetti, S. Spooner, *Phys. Rev. B* 39 (1989) 4588.